Evaluation of new materials for plasmonic imaging lithography at 476 nm using near field scanning optical microscopy

Scott A. Backer, Itai Suez, Zachary M. Fresco, and Jean M. J. Fréchet[a)]
College of Chemistry, University of California, Berkeley, California 94720-1460

Josh A. Conway, Shantha Vedantam, Hyojune Lee, and Eli Yablonovitch
Department of Electrical Engineering, University of California, Los Angeles, California 90095

(Received 9 August 2006; accepted 18 June 2007; published 26 July 2007)

A new resist formulation was successfully patterned using near field optical microscopy in order to simulate the conditions prevailing in silver based plasmonic imaging tools. Radiation at 476 nm was transmitted through a near field scanning optical microscopy fiber probe tip to cross-link a film of poly(4-methacrylmethyl styrene) via polymerization of pendant methacryloyl groups using camphorquinone and dimethyl aniline as an initiating system. Patterns were generated by scanning at several speeds in order to moderate the dose while maintaining a constant probe height of about 5 nm above the sample through shear force feedback. After development, lines corresponding to the exposed regions were observed. At a scanning speed of 4 μm/s, the observed pattern has a full width at half maximum of 275 nm and a height of ~25 nm. © *2007 American Vacuum Society.* [DOI: 10.1116/1.2757184]

I. INTRODUCTION

In standard photolithography, the wavelength of the exposure step dictates the chemical and material requirements of the resist. Each successive decrease in exposure wavelength introduces new issues in the process engineering, base line chemistry,[1] and optical materials used in the exposure system. Chemically amplified 248 nm resists such as those derived from the original *t*-butyloxycarbonyloxy-styrene system,[2–4] while still the workhorse of photolithography, do not have the transparency required to be used with the ArF laser. This has led to the development of analogous chemically amplified resists based on functionalized cyclic aliphatic hydrocarbons for 193 nm exposures[5–7] and the fluorinated derivatives required for 157 nm.[8–10]

The diffraction limit has historically forced a decrease in exposure wavelengths to reduce the critical dimension of new lithographic processes.[11,12] However, current advances in surface plasmon optics have created a new path to nanolithography. Surface plasmons are collective electron oscillations at optical frequencies confined to the surface of a conductor.[13] These modes arise classically out of Maxwell's equations and occur at the interface of a material having a positive dielectric constant with that of a material with a negative dielectric constant. The utility of surface plasmons lies in their unique dispersion relations. With the proper choice of materials and geometry,[14–16] surface plasmons can achieve incredibly short wavelengths[17] with optical frequencies. Schemes for plasmonic focusing may then exploit these large wave vectors to create deeply subwavelength critical dimensions without violating the Rayleigh criterion.[18]

This will allow for a next-generation lithography using convenient and established visible laser systems. Replacing the expensive excimer lasers with conventional diode lasers has the potential to dramatically lower the economic barrier to entry for cutting edge circuit production in both equipment and photomasks. To take advantage of this new technology, a variety of material properties including composition of the exposure tool, exposure frequencies, and resist formulation must be evaluated.

Although surface plasmons can lead to deeply subwavelength focusing, these modes tend to be subject to significant losses. Typical surface plasmon decay lengths are less than 10 μm (Ref. 19) with the majority of losses due to absorption in the metal. This intrinsic absorption mechanism puts a strong constraint on the design of any plasmonic device. To achieve even modest levels of efficiency employing surface plasmons requires careful selection of materials and optical frequencies.

We define the material quality factor (Q) of the metal to quantify the performance of various metals and frequencies for supporting plasmon waves. To determine the Q of a metal, we begin with Eq. (1), which yields the energy (U) of an electromagnetic field in a dispersive medium,[20,21]

$$U = \frac{1}{2}\int \left(\frac{\partial(\omega\varepsilon')}{\partial\omega} E^2 + \frac{\partial(\omega\mu')}{\partial\omega} H^2 \right) d\tau. \tag{1}$$

Here ε' is the real component of the relative permittivity, E is the electric field amplitude, ω is the frequency, μ' is the real component of the relative permeability, and H is the magnetic field amplitude. Unlike free space optical waves, the majority of the energy of the large wave-vector surface plasmon lies in the electric field, allowing us to drop the second term, which represents the energy stored in the magnetic field. This is to be expected in the electrostatic regime.

The average heat evolved in the material per unit time in the medium[21] is

[a)]Electronic mail: frechet@berkeley.edu

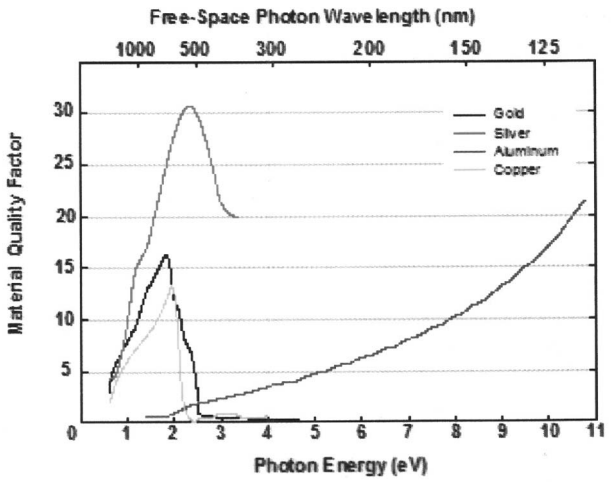

FIG. 1. Evaluation of conductors for plasmonic imaging lithography. The metal with the highest material quality factor, silver, has a peak at 2.5 eV, corresponding to optimal exposure wavelengths of 620–460 nm.

$$\frac{dU}{dt} = \omega \int (\varepsilon'' E^2 + \mu'' H^2) d\tau, \tag{2}$$

where ε'' and μ'' are the imaginary components of the relative permittivity and permeability, respectively. At optical frequencies, the imaginary component of the permeability tends to zero. This removes the magnetic term from Eq. (2). With these pieces in place, it remains to define the material Q factor[22] as a function of frequency,

$$Q \equiv \omega_0 \frac{U}{-dU/dt} = \frac{\frac{1}{2}\int ([\partial(\omega\varepsilon')/\partial\omega]E^2 + [\partial(\omega\mu')/\partial\omega]H^2) d\tau}{\int (\varepsilon'' E^2 + \mu'' H^2) d\tau} \approx \frac{1}{2\varepsilon''}\frac{\partial(\omega\varepsilon')}{\partial\omega}. \tag{3}$$

We can now evaluate metallic Q factors for various high-conductivity metals. The empirically derived dielectric constants of silver,[23–26] gold,[27] aluminum,[28] and copper[27] were used to evaluate candidate metals for possible plasmonic exposure tools. The results of these calculations are plotted in Fig. 1 and reveal that silver is the best candidate material for efficient visible exposures, having the highest metallic Q factor ($\sim$30) at $\sim$2.5 eV. We see that these considerations compel the development of a resist that can be exposed in this long-wavelength regime. Herein we report the near field visible exposure of a novel negative tone resist based on the classical photoinduced cross-linking of pendant methacryl groups on a polystyrene resin.

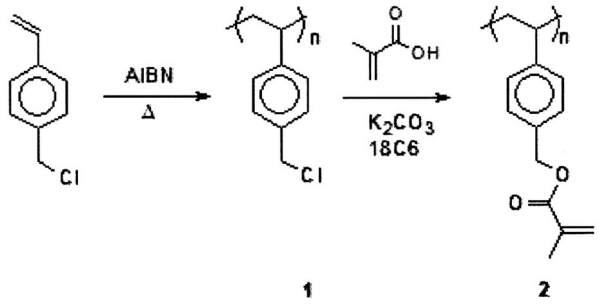

SCHEME 1. Preparation of polymer 2, poly(4-methacrylmethyl styrene).

II. EXPERIMENTAL SECTION

A. Polymer synthesis

10.8 g of 4-chloromethyl styrene was placed in a dry 50 ml Erlenmeyer flask under argon atmosphere. 10 ml of toluene and 580 mg of azobisisobutyronitrile (AIBN) were added to the flask and the solution was degassed under positive argon pressure for 30 min. The degassed solution was placed in an oil bath preheated to 73 °C and allowed to stir for 24 h. Once cooled to room temperature, the crude mixture containing polymer 1 (see Scheme 1) was added to a 500 ml Erlenmeyer flask containing 12.9 g of methacrylic acid, 41.4 g of potassium carbonate, and 300 ml of acetone. After addition of 7.9 g of 18-Crown-6, a slow evolution of gas was observed as the reaction proceeded. Upon completion, the solvent was removed under reduced pressure, and the material was extracted three times with dichloromethane from 200 ml of de-ionized water. The crude polymer 2 was then precipitated twice into 9:1 methanol:acetone and dried *in vacuo* to give 6.6 g (46% yield over two steps) of polymer 2. Size exclusion chromatography with tetrahydrofuran eluent gave the following molecular weight data for polymer 2: M_n=9.68 kDa, M_w=18.99 kDa, and polydispersity index (PDI)=2.05. NMR analysis was consistent with the expected structure for polymer 2; infrared analysis: 2926, 2536, 1717, 1448, 1158, and 815 cm^{-1}.

B. Patterning

Samples were prepared by first placing 0.5×0.5 cm^2 silicon wafers in HF, followed by oxidation by O_2 plasma with RF power of 100 W. The samples were then placed in vials containing a 10 mM solution of 2-(methacryloyloxy)ethyl [3-(triethoxysilyl)propyl]carbamate[29] under nitrogen atmosphere for 12 h to form a delaminating layer. A resist formulation consisting 50 mg of polymer 2, 30 mg of dimethyl aniline, and 30 mg of camphorquinone was dissolved in 1 ml of anisole. The samples were rinsed with acetone, methanol, and isopropanol, then dried with nitrogen before the resist was spun coat on the sample at a spin speed of 7000 rpm. Films of a thickness of $\sim$50 nm were reproducibly achieved under these conditions.

Patterning was achieved using 476 nm laser light generated by an Ar ion laser fiber coupled into a commercially available near field scanning optical microscopy (NSOM)

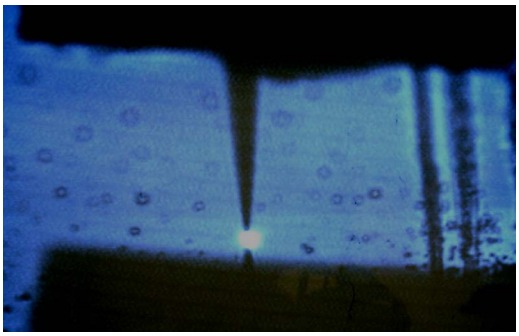

FIG. 2. Optical micrograph of the patterning step as the resist is exposed.

fiber probe tip with 80 nm internal aperture (Fig. 2). The laser power at this wavelength is 6.7 mW and the pulled-fiber NSOM probes were characterized by their far-field power loss of 50–60 dB. The fiber probe was maintained above the sample via shear force feedback at a height of about 5 nm, where the near field intensity of the light in the proximity of the tip apex is expected to be very high. The probe was scanned at several predetermined speeds, and the laser shutter was opened and closed to expose single-pass lines on the sample with a pitch of ~15 μm. Varying the probe scan speed during the patterning step controlled the exposure dose of individual lines. After exposure, the sample was developed in anisole for 20 s to remove the non-cross-linked polymer. After development, the sample was washed in acetone and 2-propanol, dried, and baked at 90 °C.

III. RESULTS AND DISCUSSION

Light induced fabrication of polymeric structures has previously been routinely achieved via radical cross-linking reactions of both multifunctional liquid resins and polymers containing pendant vinyl groups that can be polymerized using a variety of initiator systems.[11] Camphorquinone absorbs light in the 400–500 nm region and, when paired with an appropriate hydrogen donor, forms an inert ketyl radical and an amine radical capable of initiating the polymerization of suitable vinyl monomers.[30,31] The use of camphorquinone to efficiently form solid polymeric structures from liquid resins has been extensively studied[32] and used commercially for the UV curing of dental formulations.

The polymeric component of the resist we prepared is a polystyrene derivative with pendant methacrylate moieties capable of cross-linking via a radical polymerization initiated by the camphorquinone/amine system. Polymer 2 was prepared in two steps from chloromethyl styrene (Scheme 1). Free radical polymerization with AIBN as the initiator was used to prepare poly(4-chloromethyl styrene), polymer 1, which was then treated with methacrylic acid and potassium carbonate to give poly(4-methacrylmethyl styrene), polymer 2. Films were made using a mixture of polymer 2 with camphorquinone and dimethylaniline as the hydrogen donor. Relatively high concentrations of initiator were used to form enough active radicals to efficiently cross-link the film during patterning exposure (Scheme 2).

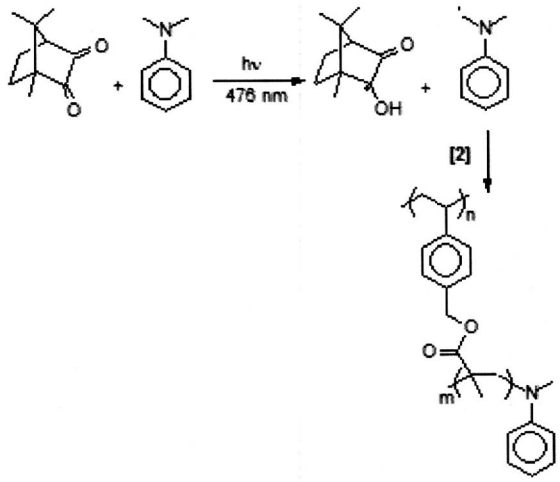

SCHEME 2. Mechanism of photoinduced cross-linking of the resist system. Excitation of camphorquinone at 476 nm ($n \rightarrow \pi^*$) followed by hydrogen abstraction from dimethylaniline initiates polymerization of poly(4-methacrylmethyl styrene) in the film, forming insoluble material in the exposed region.

After development, the samples were imaged via atomic force microscopy (Nanoscope® IIIa Digital Instruments, Santa Barbara, CA) to evaluate the patterning. Figure 3(a) shows several patterns for which exposures were performed at 4, 8, and 16 μm/s. As the exposure dose is decreased, the extent of the cross-linking reaction within the resist film is decreased with the appearance of more diffuse patterns at higher speeds, as is observed in Fig. 3(a). At 4 μm/s, lines were observed with a full width half maximum (FWHM) of 275 nm and a height of 25 nm [Fig. 3(b)]. Increasing the exposure dose further with this resist formulation led to image blur, possibly due to uncontrolled photopolymerization

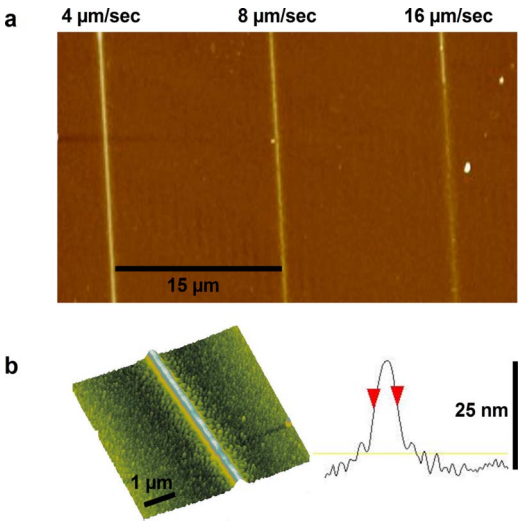

FIG. 3. (a) AFM image of the sample postdevelopment. The patterns were exposed at scan speeds of 4, 8, and 16 μm/s. The patterns become less defined as the dose is decreased from left to right, indicating a lower degree of cross-linking in the respective regions. (b) Three-dimensional AFM image of the well-defined line patterned at 4 μm/s with cross-sectional analysis. The line has a FWHM of 275 nm and a height of ~25 nm

induced by far-field effects or polymerization in the "unexposed" region, a common source of blur for negative tone lithographic systems based on cross-linking. While the film thickness of the samples was measured to be 50 nm, the patterned features observed in Fig. 3 exhibit a height of only ~25 nm. We believe that this is due to the permeability of the film to oxygen, which is more extensive near the surface and prevents effective polymerization in oxygen-exposed areas.[33]

IV. CONCLUSIONS

A resist formulation capable of exposure via visible wavelength NSOM was designed, synthesized, and tested. Initial results using an argon ion laser fiber coupled into a NSOM fiber probe tip proved that patterning could be achieved using visible radiation with resolutions well below the exposure wavelength. Patterns fabricated with a 6.7 mW laser at a tip speed of 4 μm/s exhibited a height of 25 nm and a FWHM of 275 nm. These results represent an important first step in the development of materials for plasmonic imaging lithography. It is expected that further advances in this emerging field will derive from optimization of the patterning tools the control of the environment within the exposure tool and the resist material itself.

ACKNOWLEDGMENTS

The authors thank the Center for Scaleable Integrated Nanomanufacturing (SINAM) funded by a grant of the National Science Foundation and SRC/DARPA for the support of this research.

[1]T. Bloomstein, M. Rothchild, R. Kunz, D. Hardy, R. Goodman, and S. Palmucci, J. Vac. Sci. Technol. B **16**, 3154 (1998).
[2]C. G. Willson, H. Ito, J. M. J. Fréchet, T. G. Tessier, and F. M. Houlihan, J. Electrochem. Soc. **133**, 181 (1986).
[3]J. Fréchet, C. Willson, and H. Ito, U.S. Patent No. 4,491,628 (1 January 1985).
[4]S. A. MacDonald, C. Willson, and J. Fréchet, Acc. Chem. Res. **27**, 151 (1994).
[5]J. M. Klopp, D. Pasini, J. d. Byers, C. G. Willson, and J. M. J. Fréchet, Chem. Mater. **13**, 4147 (2001).
[6]Q. J. Niu and J. M. J. Fréchet, Angew. Chem., Int. Ed. **37**, 667 (1998).
[7]R. P. Meagley, D. Pasini, L. Y. Park, and J. M. J. Fréchet, Chem. Commun. (Cambridge) **1999**, 1587.
[8]R. Kunz, T. Bloomstein, D. HArdy, R. Goodman, D. Downs, and J. Curtin, J. Vac. Sci. Technol. B **17**, 3261 (1999).
[9]H. V. Tran *et al.*, Macromolecules **35**, 6539 (2002).
[10]Z. M. Fresco, N. Bensel, I. Suez, S. A. Backer, and J. M. J. Fréchet, J. Photopolym. Sci. Technol. **16**, 27 (2003).
[11]L. F. Thompson, C. G. Willson, and M. J. Bowden, *Introduction to Microlithography*, 2nd ed. (American Chemical Society, Washington, D.C., 1994), p. 10.
[12]D. Giancoli, *Physics: Principles with Applications*, 4th ed. (Prentice-Hall, Englewood Cliffs, NJ, 1995), p. 206.
[13]H. Raether, *Surface Plasmons*, Springer Tracts in Modern Physics, Vol. 111 (Springer, New York, 1988), p. 4.
[14]E. N. Economou, Phys. Rev. **182**, 539 (1969).
[15]J. Takahara, S. Yamagishi, H. Taki, A. Morimoto, and T. Kobayashi, Opt. Lett. **22**, 475 (1997).
[16]T. Ono, M. Esashi, H. Yamada, Y. Sugawara, J. Takahara, and K. Hane, *Nano-Optics: Integrated and Functional Probes* (Springer, New York, 2001), Chap. 5, p. 130.
[17]H. T. Miyazaki and Y. Kurokawa, Phys. Rev. Lett. **96**, 097401 (2006).
[18]J. W. Strutt, Philos. Mag. **8**, 261 (1879).
[19]N. Kroo, J. P. Thost, M. Volcker, W. Krieger, and H. Walther, Europhys. Lett. **15**, 289 (1991).
[20]R. E. Collin, *Field Theory of Guided Waves* (IEEE, New York, 1991), p. 10.
[21]E. M. Lifshitz, L. D. Landau, and L. P. Pitaevskii, *Electrodynamics of Continuous Media* (Butterworth Heineman, Oxford, 2002), Vol. 8, p. 275.
[22]J. T. Verdeyen, *Laser Electronics* (Prentice Hall, Upper Saddle River, 2000), p. 153.
[23]L. G. Schulz, J. Opt. Soc. Am. **44**, 357 (1954).
[24]L. G. Schulz and F. R. Tangherlini, J. Opt. Soc. Am. **44**, 362 (1954).
[25]V. G. Padalka and I. N. Shklyarevskii, Opt. Spectrosc. U.S.S.R. **11**, 527 (1961).
[26]R. Philip and J. Trompette, Compt. Rend. **241**, 627 (1955).
[27]P. B. Johnson and R. W. Christy, Phys. Rev. B **6**, 4370 (1972).
[28]E. Palik, *Handbook of Optical Constants of Solids* (Academic, New York, 1985), p. 396.
[29]C. F. Norman, M. D. Swan, and W. E. Bottomley, U.S. Patent No. 19,960,412 (1996).
[30]Q. Yu, S. Nauman, J. P. Santerre, and S. J. Zhu, J. Appl. Polym. Sci. **82**, 1107 (2001).
[31]J. Nie, E. Andrzejewska, J. F. Rabek, L. Linden, J. P. Fouassier, J. Paczkowski, F. Scigalski, and A. Wrzyszczysnski, Macromol. Chem. Phys. **200**, 1692 (1999).
[32]A. Revzin, R. J. Russel, V. K. Yadavalli, W. Koh, C. Deister, D. D. Hile, M. B. Mellot, and M. V. Pishko, Langmuir **17**, 5440 (2001).
[33]J. Nie, L. Linden, J. F. Rabek, J. P. Fouassier, J. Paczkowski, F. Scigalski, A. Wrzysczynski, and E. Andrzejewski, Acta Polym. **49**, 145 (1998).